eXPRESS Polymer Letters Vol.15, No.12 (2021) 1174–1188
Available online at www.expresspolymlett.com
https://doi.org/10.3144/expresspolymlett.2021.94

Spiroorthocarbonate as shrinkage resistance for UV-curing 3D printing: UV-curing kinetics, mechanical properties and volume shrinkage

*G. H. Lin, L. J. Li, H. Xiang, J. Ye, H. P . Xiang, Z. Q. Li, X. X. Liu**

Guangdong Provincial Key Laboratory of Functional Soft Condensed Matter, School of Materials and Energy, Guangdong University of Technology, 510006 Guangzhou, P. R. China

Received 22 May 2021; accepted in revised form 19 July 2021

Abstract. Spiroorthocarbonates (SOCs) exhibit good shrinkage resistance with ring-opening polymerization initiated by a cationic photoinitiator, with potential application in reducing the volume shrinkage by C=C double bond polymerization on three-dimensional (3D) printing. However, SOCs as an additive dealing with volume shrinkage in 3D printing are rarely reported. Moreover, little progress has been made in the kinetics study on its ring-opening polymerization. In this study, we presented an effective strategy to reduce 3D printing volume shrinkage based on SOCs chemistry and systematically studied the ring-opening photopolymerization kinetics. 3,9-diethyl-3,9-bis(allyloxymethyl)-1,5,7,11-tetraoxastetraoxaspiro undecane (DB-TOSU), one kind of SOCs, was adopted as an expanding monomer. Initiated by cationic photoinitiator with sensitizer under 405 nm LED light, the maximum conversion of DB-TOSU is up to 84%. As a volume-control agent for 3D printing, volume shrinkage reduction is 71.2% when adding DB-TOSU into 3D printing resin based on SOCs chemistry. Moreover, the toughness of resin was enhanced. In the 3D printing application test, DB-TOSU displayed a good application prospect owing to its good compatibility with the printing resin and printing accuracy after volume expansion.

Keywords: *polymer synthesis, expanding monomer, UV-curing kinetics, volume shrinkage, 3D printing*

1. Introduction

UV-curing 3D printing, owing to low energy consumption, high molding precision, and fast forming speed [1, 2], is widely used in fabricating industrial components, high-performance elastomers, biomedical materials, dental implants, and electronics [3–5]. Nevertheless, volume shrinkage caused by photosensitive resin during UV-curing limits the development of UV-curing 3D printing technology [6]. In UV-curing reactions, the formation of a crosslinked network, usually initiated by the free radical polymerization of C=C double bond, is accompanied by the generation of internal stress due to the reduction of molecular distance, leading to volume shrinkage for printed products [7, 8]. Many methods have been used to decrease the volume shrinkage after the UV-curing reaction. Traditionally, incorporation of cationic curing components and free radical curing components to fabricate hybrid UV-curing systems [9–11] to reduce the concentration of C=C double bonds is a simple and effective measure suppressing the internal stress because cationic UV-curing leads to a smaller volume shrinkage compared with free-radical curing [8, 12]. However, the curing rate of hybrid UV-curing systems slows down the curing rate due to a slower cationic UV-curing rate compared with free radical curing, which is not conducive to 3D printing applications. Thiol-ene photopolymerization exhibits low volume shrinkage because of delayed gel point and homogeneous network in 3D printing

*Corresponding author, e-mail: p_xxliu@aliyun.com

application [13, 14]. But the possibility of UV curing without photoinitiator goes against long-term storage [15], and a single thiol-ene system is not conducive to the wide range of UV curing 3D printing. Other methods, such as introducing sterically hindered groups or inorganic fillers [16, 17], need consideration for increased viscosity, uneven dispersion, weak interlayer adhesion during 3D molding [18].

Incorporating shrinkage resistance monomers like vinylcyclopropane (VCP) [19], vinyl sulfonate esters [20], expanding monomer [21], and so on is a new strategy to lower the shrinkage in UV-curing 3D printing. Expanding monomers exhibiting volume expansion during UV-curing, unlike most shrinkage resistance monomers, have attracted much attention in recent years due to high curing reactivity and possibilities for tailoring. Spiroorthoesters (SOEs) and spiroorthocarbonates (SOCs) are the most widely studied expanding monomers. SOCs are more widely applied in the industrial field since the performance of these monomers exceeds that of SOEs [21]. The polymerization mechanism includes nucleophilic addition of a cationic photoinitiator to a SOCs molecule, leading to the generation of a carbocation which reacts with another SOCs molecule to achieve chain growth in the ring-opening photopolymerization [22]. The broken C–O bonds are converted into C=O bonds, and the double ring-opening polymerization of SOCs produces poly(ether carbonates). In a crosslinking network, flexible molecular chains, *i.e.*, poly (ether carbonates), can effectively offset the internal shrinkage stress in the polymeric matrix. Hence, the volume expansion effect caused by SOCs will reduce the volume shrinkage during UV-curing. Many studies have been reported to prove the effectiveness of SOCs. Sangermano *et al*. [23] successfully prepared an epoxy-functionalized SOCs, which expands the volume after polymerization in the presence of 10 wt% of functionalized SOCs. Ortiz *et al*. [24] reported a diol SOCs (DIOL SOCs) as an antishrinkage additive for cationic photopolymerization. At 20 mol% dosage, the volume shrinkage was reduced by 45%. Moreover, they modified DIOL SOCs to functionalize with allylic groups (SOCs DA) to reduce the shrinkage of a typical dental resin [25]. Min *et al*. [26] added 3,9-diethyl-3,9-bis(allyloxymethyl)-1,5,7,11-tetraoxastetraoxaspiro undecane (DB-TOSU) to the matrix resin to apply for UV nanoimprint lithography (UV-NIL). When DB-TOSU reached 50 wt%, the volume shrinkage decreased to 1.86%. Until now, the number of studies focusing on the expanding monomers applied in 3D printings is quite limited and only one reported the less popularly used SOEs as an additive for shrinkage resistance [27], proving that expanding monomer has potential to reduce Digital Light Procession (DLP) 3D printing volume shrinkage. Moreover, little progress has been made in the kinetics study on the ring-opening polymerization of SOCs. In this study, we presented an effective strategy to reduce UV-curing 3D printing volume shrinkage based on SOCs chemistry and systematically studied the ring-opening photopolymerization kinetics. 3,9-diethyl-3,9-bis(allyloxymethyl)-1,5,7,11-tetraoxastetraoxaspiro undecane (DB-TOSU), one kind of SOCs, was adopted as an expanding monomer. The initiation efficiency of different types and dosages of the cationic initiators was investigated by real-time Fourier transfer infrared (RT-FTIR) spectroscopy. To make it suitable for 3D printing applications, the photosensitization effect of different types of photosensitizers to sensitize cationic initiating systems were studied as well. Moreover, the potential function of DB-TOSU in 3D printing was developed. By conducting volume shrinkage tests, the optimal amount of expanding monomer addition to a 3D printing resin was selected. The mechanical properties and microstructure morphology of DB-TOSU and its application in 3D printing were analyzed.

2. Experimental

2.1. Materials

Tetraethyl orthocarbonate was purchased from Beihe Chemical, Shanghai, China. Trimethylolpropane allyl ether was purchased from Sigma-Aldrich, Shanghai, China. Triethylamine, toluene, dichloromethane (CH_2Cl_2), acetonitrile and *p*-toluenesulfonic acid (*p*-TsOH) were purchased from Damao Chemical Reagent Factory, Tianjin, China. Free radical initiator TPO-L and cationic initiators, IRGACURE 261, IRGACURE 204s, and IRGACURE 205, were obtained from Polynaisse Resources Chemicals, Shanghai, China. UVI 6992 was purchased from Nantong Synasia New material, Jiangsu, China. All the photoinitiators are shown in Figure 1. The photosensitive resin for 3D printing was prepared in advance according to the formula. Perylene and Sudan III were purchased from Aladdin Biochemical Technology, Shanghai, China. Curcumin was obtained from Macklin Biochemical, Shanghai, and 2-isopropyl

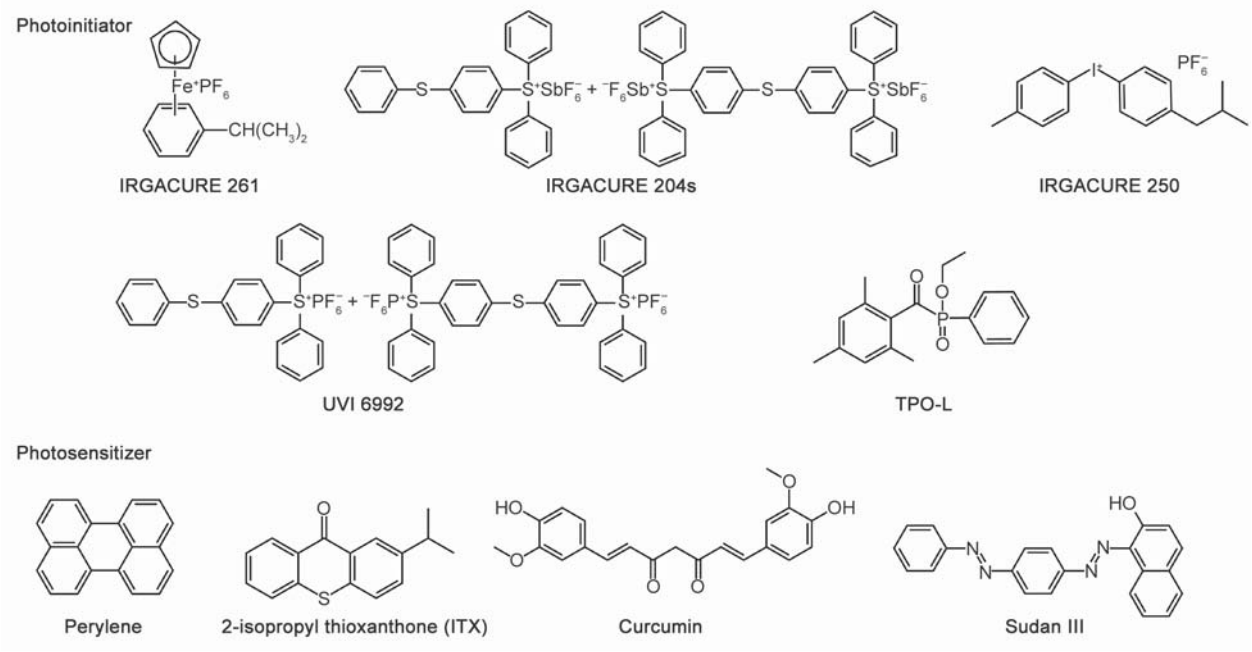

Figure 1. Chemical structures of the cationic photoinitiators and photosensitizers used in this study.

thioxanthone (ITX) was supported by Polynaisse Resources Chemicals, Shanghai, China.

2.2. Synthesis of DB-TOSU

According to a previous study [26], the expanding monomer DB-TOSU was synthesized by the transesterification reaction between tetraethyl orthocarbonate and trimethylolpropane allyl ether. In a four-necked round-bottom flask equipped with a mixer, nitrogen inlet, thermometer, and water separator, 43.56 g (0.25 mol) of trimethylolpropane allyl ether and 300 ml of toluene were refluxed to remove water at a temperature of 115 °C for 2 h. Then, 0.42 g of *p*-TsOH was slowly added until the pot temperature decreased to 70 °C or less. During cooling to room temperature, 24.03 g (0.125 mol) of tetraethyl orthocarbonate was added dropwise. The transesterification reaction was carried out at 115 °C. A synthetic route for the expanding monomer DB-TOSU is shown in Figure 2a.

The reaction was terminated after 3 h; then, 20 ml of triethylamine was added. A yellow liquid was obtained after distilling using a rotary evaporator. The transparent liquid was purified by thin-layer chromatography (TLC) using silica gel as the stationary phase and petroleum ether: ethyl acetate (90:10 v/v) as the eluent.

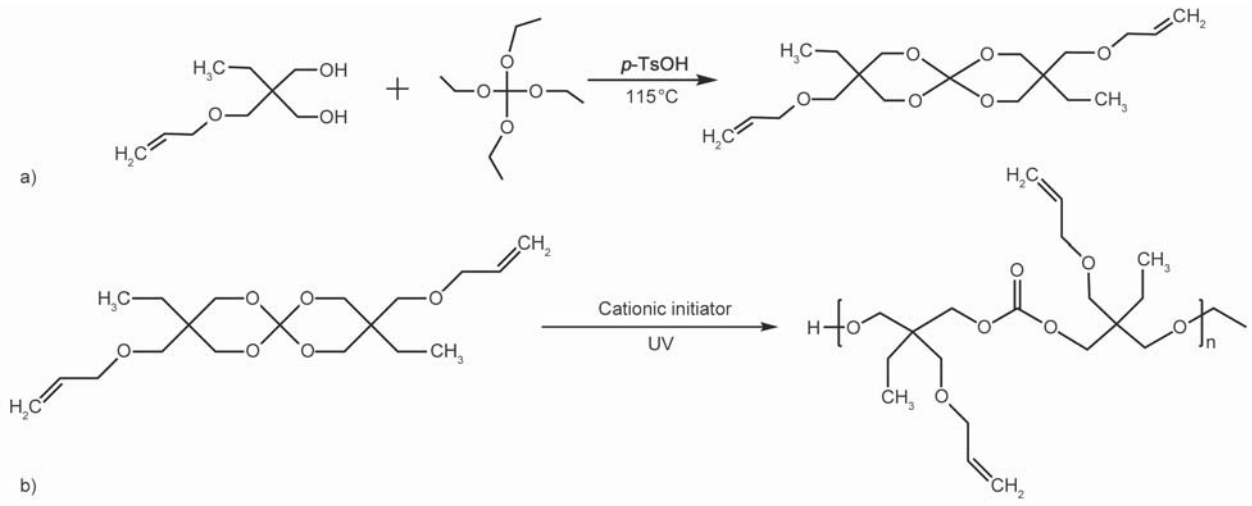

Figure 2. (a) Synthetic routes of expanding monomer DB-TOSU; (b) double ring-opening polymerization mechanism of DB-TOSU.

2.3. Preparation of 3D printing resin with the expanding monomer DB-TOSU

A self-made photosensitive 3D printing resin was prepared according to the formula shown in Table 1. Expanding monomer DB-TOSU was added in the range of 10~40 wt% with respect to the total amount of photosensitive 3D printing resin. After the photosensitive 3D printing resin was mixed well with DB-TOSU, a mixture of cationic photoinitiator, photosensitizers, and radical photoinitiator TPO-L was added to all the formulas. After complete dissolution, the resin was defoamed in vacuum and stored in a dark place.

2.4. Characterization

Fourier transform infrared (FTIR) spectroscopy was carried out using an IS-50 Nicolet FTIR spectrometer, Thermo Fisher, Germany. The liquid expanding monomer DB-TOSU was coated on a KBr disc. The absorbance was measured at a resolution of 4 cm^{-1} in the 400–4000 cm^{-1} wavenumber region and each spectrum was an average of 32 scans. To further prove that DB-TOSU performs a ring-opening reaction after UV-curing, 5 wt% cationic photoinitiator IRGACURE 204s was added into DB-TOSU. The sample coated on a KBr disc was exposed to LED light for 5 min. After that, the absorbance of the sample was measured as well.

Real-time FTIR (RT-FTIR) was carried out using an IS-50 Nicolet FTIR spectrometer, Thermo Fisher, Germany, equipped with a LED UV light source. DB-TOSU with a cationic photoinitiator and 3D printing resin were coated on a KBr disc with a thickness of 50 μm and then *in situ* irradiated with a 405 nm LED light source with an intensity of 100 mW/cm^2. Each spectrum obtained from the IR spectrometer was an average of 4 scans with a resolution of 8 cm^{-1}. The CH_2 peak at 2980 cm^{-1} was selected as the internal standard as it remained constant during the UV measurement. The peak of spiro group at 1205 cm^{-1} and peak of C=C double bond at 810 cm^{-1} were used to determine their conversion (C) according to Equations (1) and (2) [28]:

$$C(\text{spiro}) = \frac{\frac{A_{0_{1205\ cm^{-1}}}}{A_{0_{2980\ cm^{-1}}}} - \frac{A_{1_{1205\ cm^{-1}}}}{A_{1_{2980\ cm^{-1}}}}}{\frac{A_{0_{1205\ cm^{-1}}}}{A_{0_{2980\ cm^{-1}}}}} \quad (1)$$

$$C(\text{C}=\text{C}) = \frac{\frac{A_{0_{810\ cm^{-1}}}}{A_{0_{2980\ cm^{-1}}}} - \frac{A_{1_{810\ cm^{-1}}}}{A_{1_{2980\ cm^{-1}}}}}{\frac{A_{0_{810\ cm^{-1}}}}{A_{0_{2980\ cm^{-1}}}}} \cdot 100\% \quad (2)$$

where C(spiro) is the conversion of spiro group during the polymerization; C(C=C) is the conversion of the double bond of 3D printing resin during UV-curing; A_0 is the integral area of the related peaks before

Table 1. Formula of 3D printing resin.

Prepolymer	Chemical stucture	Quality [g]	Purchased from
Isobornyl acrylate (IBOA)	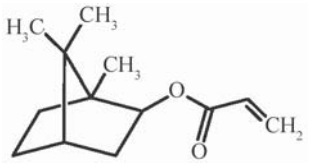	100	Germany RYOJI Chemistry, Shanghai, China
Di(trimethylolpropane) tetraacrylate (DTMPTTA)	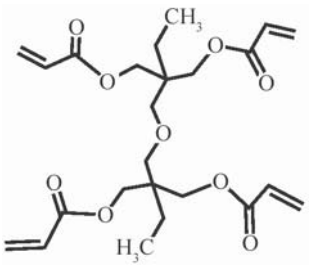	50	Z&D Chemical, Shanghai, China
Aliphatic polyurethane diacrylate oligomer (PHOTOMER 6891)	–	50	IGM Resins Management Co., Ltd., Shanghai, China
Polyurethane acrylate oligomer (RUA 048)	–	20	Asia Industry Co.,Ltd, Tokyo, Japan
2-Hydroxyethyl acrylate (HEA)	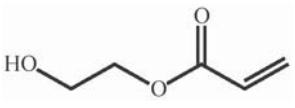	15	Aladdin Biochemical Technology, Shanghai, China

UV curing; A_1 is the integral area of the related peaks after UV-curing.

^{1}H nuclear magnetic resonance (^{1}H NMR) was measured using an AVANCE III 400 MHz Superconducting Fourier spectrometer, Bruker, Germany and chloroform as the solvent.

UV absorption spectra of the photosensitizers were obtained using a TU1810 UV–visible spectrophotometer, Beijing Purkinje General Instrument, China. The photosensitizers used in the study were dissolved to 10^{-5} mol/l in acetonitrile and photoinitiators were dissolved in acetonitrile with a concentration of 10^{-5}~10^{-3} mol/l in acetonitrile. All the samples were added to a cuvette to obtain the absorbance spectra. The absorbance was measured in the region 200–600 nm.

Tensile tests were conducted according to the ASTM D412 standard using a SANS CMT 6000 universal tester, MTS Systems Co., Ltd., America, with a crosshead speed of 10 mm/min under 25 °C. The impact strength was measured using an XBL-5.5D digital testing machine, Guangce Automation Equipment, China, according to the GBT1843-2008 standard. The hardness of the printed products were measured by a Handpi LX-D Shore D durometer, Yueqing Handpi Instruments Co., Ltd., China, according to GB/T531− 1999.

The density of samples was measured using a Specific Gravity Measurement SMK-401 instrument, Shimadzu, Japan. The specific density of the liquid resin before curing was measured directly. The specific density of the solid resin after 3D printing was measured by infiltrating in water with a density at 25 °C of $d^{25} = 0.9971$. Based on CAD model, a 20×20×10 mm cube was printed and post cured for measuring the specific density. 3D printing resins with different contents of expanding monomer were printed 3 cubes to measure for average. The specific volume shrinkage of the samples before and after curing was calculated using Equation (3) [24]:

$$\text{Volume shrinkage [\%]} = \frac{\rho_1 - \rho_0}{\rho_0} \cdot 100\% \quad (3)$$

where ρ_0 is the specific density of liquid resin before curing; ρ_1 is the specific density of solid resin after curing.

Viscosity measurements were performed by a Haake Mars rheometer system, Thermo Fisher, Germany. The measurements were conducted at 25 °C across the frequency range of 100–1000 s^{-1}.

Gel fractions of printed samples were measured in accordance with the ASTM D 2765 with a Soxhlet extractor. About 2 g 3D printing resins with different contents of expanding monomer were dissolved by CH_2Cl_2 for 24 h to analyze the gel fraction of the resins. The insoluble part was dried at 60 °C for 24 h to a constant weight. The gel fraction was calculated by the following Equation (4) [29]:

$$\text{Gel fraction [\%]} = \frac{W_1}{W_0} \cdot 100\% \quad (4)$$

where W_0 is the weight before dissolution and W_1 is the weight after dissolution.

The dynamic mechanical properties of samples were measured using a DMA-50N, MetraviB, France, in the tension mode from –50 to 200 °C at a heating rate of 3 °C/min and a frequency of 1 Hz.

The microstructure of printed products was observed using a scanning electron microscope FE-SEM SU8010, Hitachi, Japan, at an accelerating voltage of 5 kV. The printed product was frozen brittle to obtain a small part and fracture surface by liquid nitrogen. All samples were sprayed with a thin layer of gold particles to improve conductivity before scanning.

3D printing was performed on a commercially available desktop liquid crystal display (LCD) 3D printer, Weistek Technology, China, which was equipped with a LED light source (405 nm, 4 mW/cm^2). The XY pixel resolution was 1620 pixel × 2560 pixel. The layer thickness was set at 100 μm and the exposure time was 30 s. After printing, the products were washed with ethanol in order to remove the non-cured resin. After removing non-cured resin, the products were post-cured in the LED lightbox for 2 min.

3. Results and discussion

3.1. Characterization of DB-TOSU

The monomer DB-TOSU was characterized by FTIR and ^{1}H NMR analyses. Figure 3a shows the FTIR spectra of DB-TOSU. The results show the presence of C=C double bonds at 308 and 1646 cm^{-1}. A strong absorption peak between 1241 and 1149 cm^{-1} belongs to SOCs [30]. SOCs are double-cyclic acetals formed by double ring-opening polymerization initiated by a cationic photoinitiator. SOCs are converted to the carbonyl group and hydroxyl group through ring-opening photopolymerization. Thus, the peaks at 1745 and 3449 cm^{-1} belong to the newly formed carbonyl group and the hydroxyl group of the sample with a cationic photoinitiator after UV-curing.

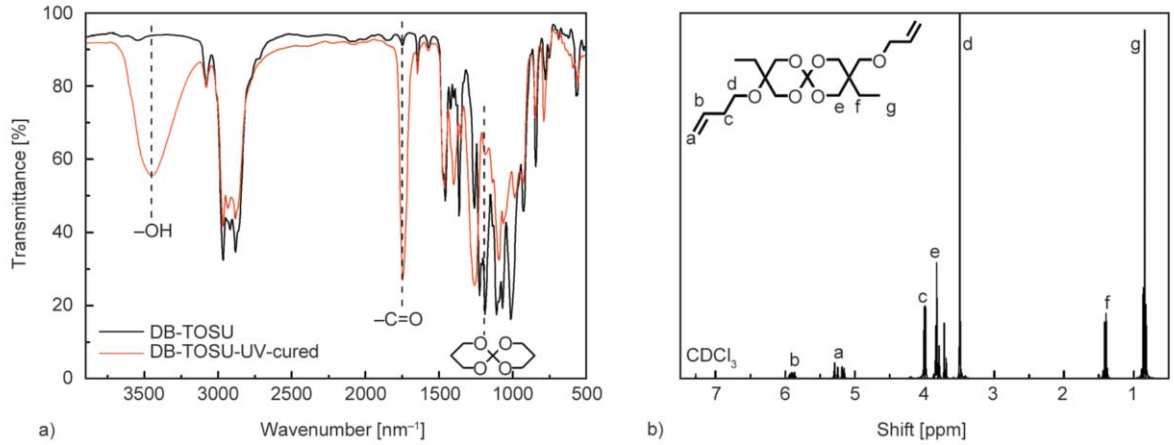

Figure 3. (a) FTIR spectra of DB-TOSU before and after UV-curing; (b) ^{1}H NMR spectrum of DB-TOSU.

Clearly, the peak between 1241 and 1149 cm^{-1} of SOCs was weakened after UV-curing, indicating that DB-TOSU can be used to perform ring-opening polymerization. Figure 3b shows the ^{1}H NMR spectrum of the synthesized DB-TOSU. All hydrogen atom signals on the spectrum are consistent with the theoretical structure. Clearly, DB-TOSU was successfully synthesized.

3.2. Kinetics of ring-opening photopolymerization of DB-TOSU

DB-TOSU is one of the expanding monomers for SOCs, and it has been well studied [22]. SOCs are double-cyclic acetals formed by double ring-opening polymerization. Initiated by a cationic photoinitiator, DB-TOSU can be used to perform ring-opening photopolymerization to produce poly(ether carbonates) [31], as shown in Figure 2b. Nevertheless, many studies paid attention to the UV-curing kinetics of photosensitive resin with SOCs. The kinetics of ring-opening photopolymerization of SOCs has rarely been reported. Hence, it is necessary to study the kinetics of ring-opening photopolymerization of DB-TOSU. As shown in Figure 1 and Figure 4a, selected photoinitiators in the study were absorbed in a concentration of 10^{-3} mol/l at 405 nm wavelength, the same as LED light. The conversion of the spiro group of ring-opening photopolymerization of DB-TOSU initiated by different cationic photoinitiators under a LED 405 nm light is shown in Figures 4b and 4c. Instantly, the ring-opening photopolymerization of DB-TOSU was trigger stimulated by an LED light. With the same dosage of 5 wt% amount, IRGACURE 261 shows an earlier initiation effect, but the conversion of the spiro group is the lowest among all the photoinitiators used. Because IRGACURE 261 is a ferrocenium salt and an attractive photoinitiator for cationic polymerization, it undergoes photolysis to generate an iron-based Lewis acid with the loss of the arene ligand [32]. However, the photolysis is usually carried out by heating the arene ligand for better triggering [33, 34]. Owing to higher reduction potentials of iodonium salts, IRGACURE 250 is much more prone to sensitization compared with the sulfonium salt [35, 36], which is consistent with stronger absorption at 405 nm in the ultraviolet spectra. However, the limiting of conversion indicates rapid consumption of the cationic photoinitiator IRGACURE 250, a similar trend of polymerization conversion can be found in previous work [36]. The samples initiated by IRGACURE 204s and UVI 6992 have the same trend during the ring-opening photopolymerization. The sample initiated by IRGACURE 204s has the highest conversion of up to 82.71% as well as the fastest rate of photopolymerization. Because the non-nucleophilic anion (SbF_6^-) of IRGACURE 204s produces a more acidic Lewis acid than the non-nucleophilic anion (PF_6^-) of UVI 6992 [37], IRGACURE 204s should be considered as a proper photoinitiator for the ring-opening photopolymerization of DB-TOSU.

The dosage of a photoinitiator is a key factor in the ring-opening photopolymerization kinetics. Figures 4d shows the effect of different dosages of IRGACURE 204s on the ring-opening photopolymerization of DB-TOSU. The start-up time of photopolymerization increases with the increase in the dosage of IRGACURE 204s from 1 to 9 wt%. With the increase in the dosage of IRGACURE 204s, the rate of photopolymerization gradually increases. 9 wt% of the dosage of IRGACURE 204s showed the fastest rate of photopolymerization rather than

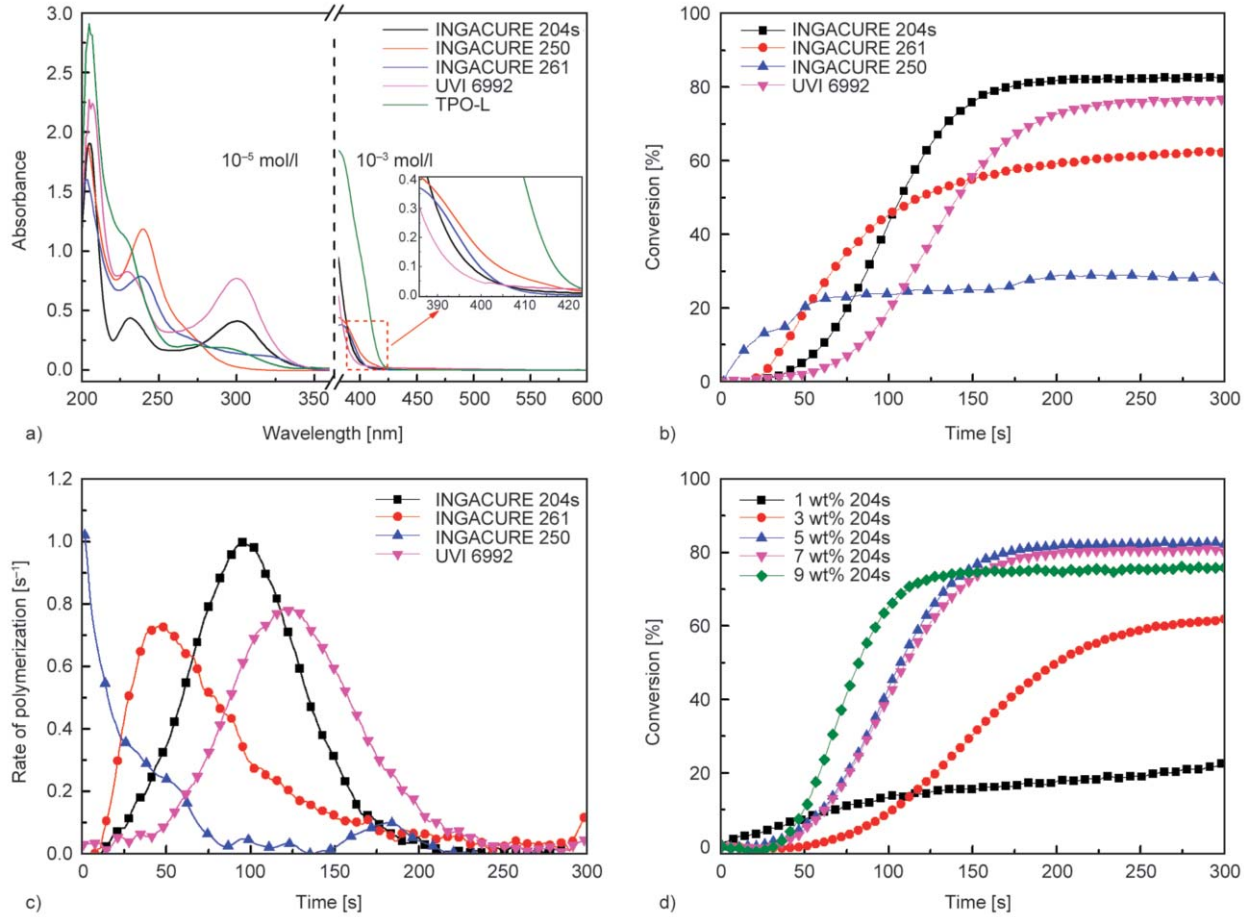

Figure 4. (a) UV absorption spectra of different photoinitiators. Effect of different cationic photoinitiators and dosage of IRGACURE 204s on the photopolymerization kinetics of DB-TOSU: (b) conversion of spiro group and (c) the rate of ring-opening photopolymerization as a function of irradiation time with different cationic photoinitiators of 5 wt%; (d) conversion of spiro group as a function of irradiation time with different dosages of IRGACURE 204s.

the highest conversion. This can be attributed to the 'cage effect' during the photolysis of the photoinitiator [38]. An increase of photoinitiator dosage will trigger prepolymer surrounding cations, which construct cage 'wall'. Scavenging of cations by a 'wall' can be observed with a degree of polymerization increase which affects the overall efficiency of photoinitiator [39]. In fact, with more than 5 wt% of dosage of IRGACURE 204s, the conversion of the spiro group started to decrease. Thus, it is more appropriate to select 5 wt% of the dosage of IRGACURE 204s to initiate the ring-opening reaction of DB-TOSU.

To make it suitable for 3D printing applications, the initiation rate of expanding monomer should be increased to reach the rate of photoinitiation of 3D printing resin, which can better improve the performance of 3D printing resin during 3D molding [40]. A reliable method is to increase the initiation rate by adding a photosensitizer [3]. As shown in Figure 1 and Figure 5a, perylene, curcumin, ITX, and Sudan III were selected as the photosensitizer, which absorbed at 405 nm wavelength, the same as LED light. Figure 5b shows the initiation effect of different photosensitizers for IRGACURE 204s. With 5 wt% dosages of IRGACURE 204s, the photosensitizers were added with a ratio of 1:10 to a dosage of IRGACURE 204s. The conversion of all the sensitized samples was maintained well, with a conversion of up to 80%. Sample initiated by ITX increased the rate of photopolymerization and had the greatest conversion improved up to 84%, but curcumin and Sudan III reduced the rate of photopolymerization. Besides, To prevent the 'absorption window' with color from photosensitizers from competing with light absorption against the free radical initiator TPO-L in the 3D printing resin [41], which affects the curing of 3D printing resin, the effect of photosensitizer on the 3D printing resin should be evaluated.

Hence, photosensitizers, perylene, and ITX, were selected to investigate the effect on 3D printing resin with a ratio 1:10 and 1:100 to the dosage of TPO-L. The conversion of C=C double bond was measured,

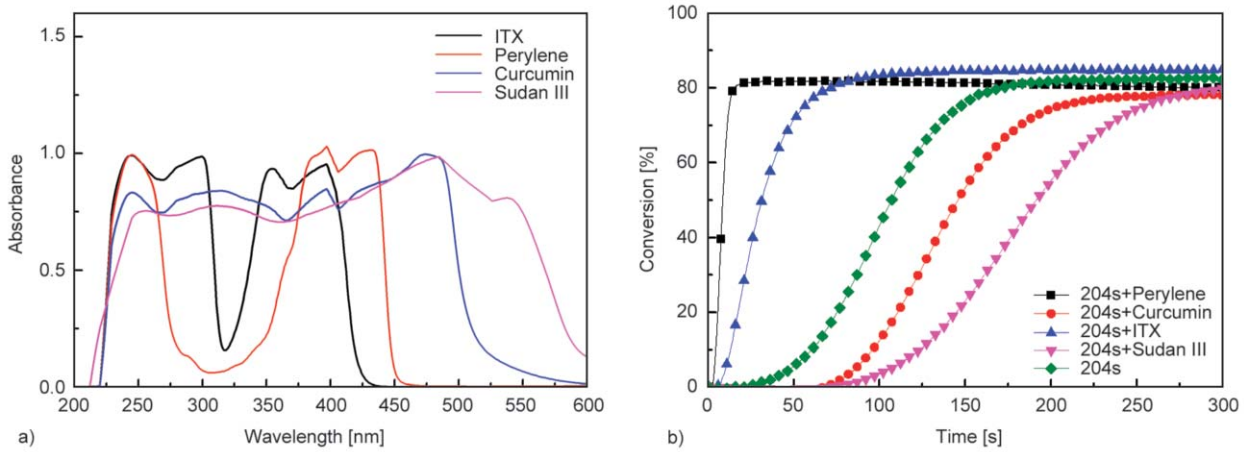

Figure 5. (a) UV absorption spectra of different photosensitizers; (b) conversion of spiro group as a function of irradiation time with different cationic photosensitizers in a ratio 1:10 to a dosage of IRGACURE 204s.

as shown in Figure 6a. When the photosensitizer was added in a small amount with a ratio of 1:100, the conversion of sample sensitized by ITX is consistent with the control sample with only TPO-L, but the conversion of sample sensitized by perylene slightly decreased. When the photosensitizer was added more with a ratio of 1:10, the conversion of sample sensitized by perylene decreased, which is only 60%,

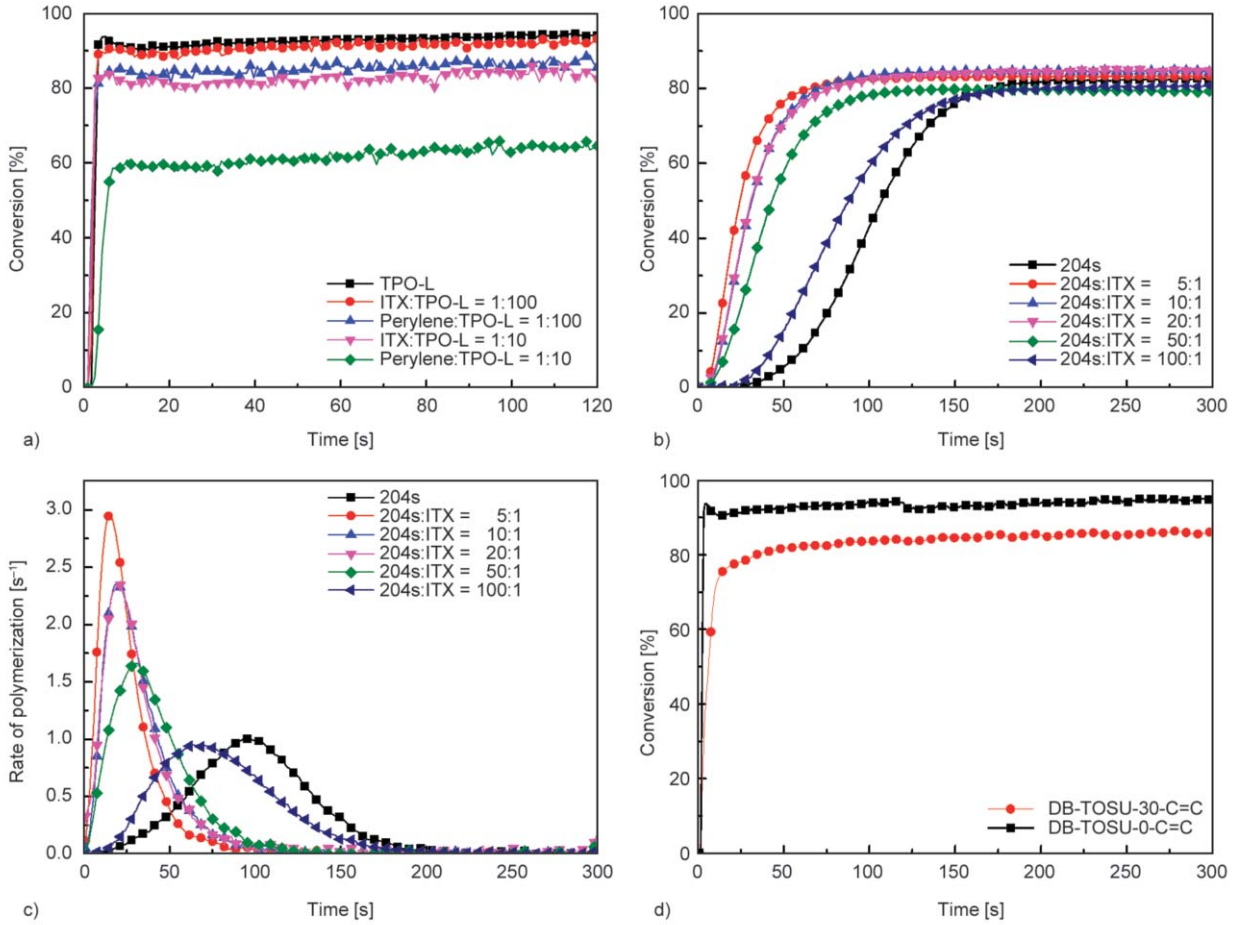

Figure 6. (a) Effect of photosensitizer on the conversion of C=C double bond of 3D printing resin. Effect of different ratios of photosensitizer ITX to IRGACURE 204s on the photopolymerization kinetics of DB-TOSU; (b) conversion of spiro group and (c) the rate of ring-opening photopolymerization as a function of irradiation time with 5 wt% IRGACURE 204s sensitized by different ratios of photosensitizer ITX. (d) Conversion of C=C double bond of 3D printing resin and C=C double bond and spiro group of 3D printing resin with expanding monomer.

while ITX does not significantly affect the resin curing. A gradual increase in the amount of perylene produced a deeper color, probably inducing the absorption, reflection, and scattering of the light leading to a reduction in the final conversion [42]. Thus, photosensitizer ITX is a better choice for sensitizing the ring-opening reaction of DB-TOSU to ensure the performance of 3D printing resin.

Different photosensitizer dosages will affect the kinetics of ring-opening photopolymerization of DB-TOSU as well. Thus, we varied the ratio of photosensitizer ITX from 1:100 to 1:5 to IRGACURE 204s to evaluate the effect of photosensitization. When using 5 wt% dosage of IRGACURE 204s, the conversion and rate of photopolymerization are shown in Figures 6b and 6c. The rate of photopolymerization and conversion increases with an increase in the dosage of photosensitizer ITX. The conversions of photopolymerization were maintained above 80%. When the dosage of ITX increased to 5:1, the conversion of the sample slightly decreased. This is probably due to a light screening effect [43]. Hence, the optimal ratio of IRGACURE 204s sensitized by ITX is 10:1.

Figure 6d shows the kinetics of photopolymerization of 3D printing resin with or without expanding monomer. The curve of resin with 30 wt% DB-TOSU has the same trend as resin without DB-TOSU. The addition of 30 wt% DB-TOSU doesn't affect the curing performance of 3D printing resin because the conversion of resin with 30 wt% DB-TOSU exceeds 80% as well as a fast curing rate. Partially reduced conversion against 3D printing resin is attributed to free vinyl of DB-TOSU in the crosslinking network.

3.3. Volume shrinkage and mechanical property of 3D printing resin with expanding monomer

After the kinetics of ring-opening photopolymerization of DB-TOSU was clarified, the efficiency of DB-TOSU as a volume-control agent was evaluated by adding to a 3D printing resin. The composition is shown in Table 2. TPO-L was added to 2 wt% of 3D printing resin, and IRGACURE 204s sensitized by ITX was added to 5 wt% of DB-TOSU.

Figure 7a and Table 3 show the effect of DB-TOSU as a volume-control agent addition to a 3D printing resin. With the increase in DB-TOSU content, the volume shrinkage of 3D printing resin significantly decreased. The volume shrinkage of the resin without DB-TOSU is 3.28%, while the volume shrinkage of the resin with 30 wt% DB-TOSU is 0.93%, which decreased to 71.2% compared with the 3D printing resin without DB-TOSU. DB-TOSU undergoes ring-opening photopolymerization initiated by cationic photoinitiators during UV curing, resulting in an expansion of the volume through the changes in chemical bond length. In the curing of acrylate monomer initiated by a free radical photoinitiator, the Van der Waals distance between the monomers changes to the length of the covalent bond between the polymers [44]. This phenomenon shortens the distance between molecular chains, causing volume shrinkage in general. However, SOCs in DB-TOSU undergo ring-opening to form C=O bond leading to an excess Van der Waals distance, which will reduce the volume shrinkage caused by acrylate monomers [45]. Nevertheless, the volume shrinkage of the resin with 40 wt% does not continue to decrease. This is because when the proportion of expanding monomers in the system is too large; a part of DB-TOSU agglomerates, resulting in the entanglement between the molecular chains preventing further expansion of the volume [46].

Moreover, with the increase in DB-TOSU, the impact strength of the cured 3D printing resin gradually increases as shown in Figure 7b. The 3D printing resin with 30 wt% DB-TOSU has a maximum impact strength of 2.20 kJ/m^2. This behavior can be attributed to the flexible effect of the polyether carbonate produced by the ring-opening polymerization of SOCs [47]. Gel fraction analysis can give further information regarding the microstructure of a crosslinked network [29]. Gel fraction of DB-TOSU

Table 2. Composition of 3D printing resins with different contents of DB-TOSU.

Sample	3D printing resin [g]	DB-TOSU [g]	TPO-L [g]	IRGACURE 204s [g]	ITX [g]	DB-TOSU content [wt%]
DB-TOSU-0	100	0	2	0.0	0.00	0
DB-TOSU-10	100	10	2	0.5	0.05	10
DB-TOSU-20	100	20	2	0.5	0.05	20
DB-TOSU-30	100	30	2	0.5	0.05	30
DB-TOSU-40	100	40	2	0.5	0.05	40

0~30 is maintained above 90%, indicating that DB-TOSU and crosslinked network constructed by 3D printing resin have good compatibility and chemical modification. Correspondingly, a slight decrease in gel fraction could be attributed to slightly reduce the crosslinking density and homogeneity with the addition of DB-TOSU. Therefore, the internal stress is effectively reduced, and the impact strength correspondingly increases. However, when the proportion of expanding monomers in the system increases to 40 wt%, agglomeration will occur, which leads to the presence of free components in the crosslinked network. Free components of DB-TOSU significantly reduced crosslinking density, weakening the crosslinking strength and increasing the chance of molecular chain entanglement [48]. Similarly, a noticeable drop in gel fraction of DB-TOSU-40, which is only 86%. The impact strength slightly decreases with 40 wt% expanding monomers added.

Tensile strength decreases with the increase in DB-TOSU content, as shown in Figure 7c. Because of flexible segments weakens the rigidity of crosslinked network consisting with a decrease of crosslinking density. In terms of physical properties, elastic modulus and hardness decrease with DB-TOSU addition presented in Table 3 as well. Particularly, with the increase of DB-TOSU content, elongation significantly increases due to the flexibility of the network giving the mobility of molecular chains. According to this, DB-TOSU-30 has the maximum impact strength as well as the largest elongation. To sum up, DB-TOSU addition slightly deteriorated the mechanical properties of the printing resin but increased impact strength, which has the same pattern in Li's work [46]. This is related to the slight decrease in the density of the crosslinking network and the introduction of flexible segments.

Viscosity is very important for the molding performance of 3D printing. As shown in Figure 7d, the viscosity of DB-TOSU is 227 mPa·s, which is much lower than some reported shrinkage resistance monomer like vinylcyclopropane (VCP) [19], and has

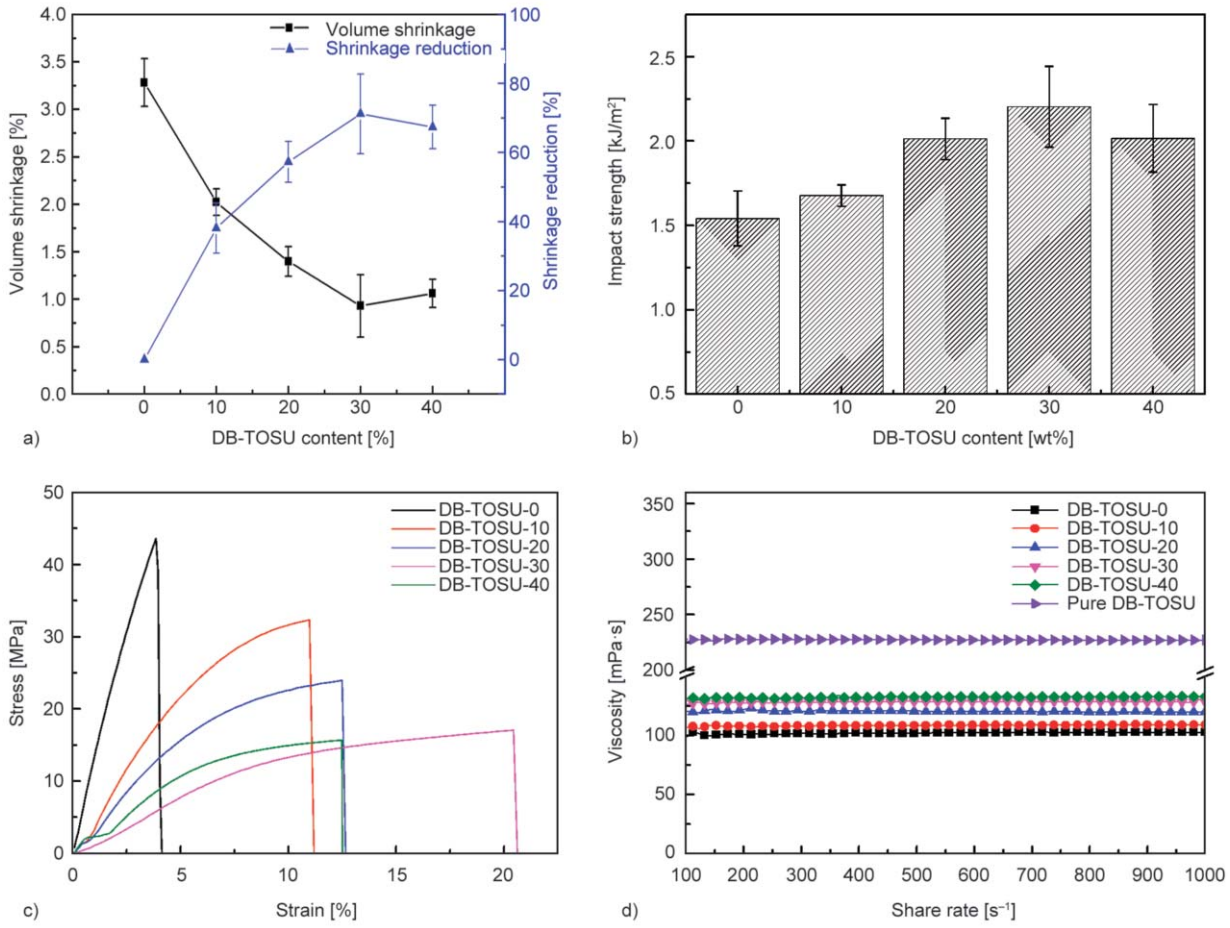

Figure 7. (a) Volume shrinkage and shrinkage reduction of 3D printing resin with different contents of DB-TOSU; (b) impact strength of 3D printing resin with different contents of DB-TOSU; (c) tensile strength of 3D printing resin with different contents of DB-TOSU; (d) viscosity of 3D printing resin with different contents of DB-TOSU.

Table 3. Comparison of the effect of the content of DB-TOSU on mechanical properties and volume shrinkage.

Sample	Impact strength [kJ/m^2]	Tensile strength [MPa]	Elastic modulus [MPa]	Volume shrinkage [%]	Shore hardness [HD]	Gel fraction [%]
DB-TOSU-0	1.54±0.16	47.35±3.57	867.20±132.92	3.28±0.25	82.5±0.3	97.41±0.29
DB-TOSU-10	1.67±0.06	33.08±0.95	670.97±74.76	2.02±0.14	81.4±0.4	95.99±0.88
DB-TOSU-20	2.01±0.12	23.66±4.87	471.44±107.34	1.40±0.16	76.7±0.6	94.12±0.39
DB-TOSU-30	2.20±0.24	18.20±6.06	449.23±85.97	0.93±0.33	64.4±0.7	92.02±0.82
DB-TOSU-40	2.02±0.20	15.24±2.37	216.41±82.69	1.06±0.15	45.1±0.7	86.48±1.57

great potential in 3D printing applications. 3D printing resin with DB-TOSU has a viscosity of less than 200 mPa·s, and the ultra-low viscosity can meet the performance requirements of 3D printing.

3.4. Dynamic mechanical property

The effect of expanding monomer DB-TOSU on the crosslinked structure of 3D printing resin was evaluated based on the storage modulus and tan δ curves obtained from dynamic mechanical analysis (DMA). As shown in Figure 8a, the storage modulus for 3D printing resin revealed a significant decrease from 1600 to 1100 MPa with increasing content of DB-TOSU. This finding is in agreement with the flexibility of polyether carbonate produced by SOCs compared with rigid networks formed by 3D printing resin [49]. In fact, a decrease of storage modulus could be related to less energy to dissipate and a decrease of crosslinking density [50]. This corresponded to the gel fraction result. The peaks of loss factor in tan δ curves reflect the glass transition temperature (T_g), presented in Figure 8b [51]. Single glass transition peak in tan δ curves was indicative of the formation of a homogeneous polymer network and good compatibility between DB-TOSU and 3D printing resin [27]. T_g of the 3D printing resin shown in Figure 8b shifted to lower temperatures when DB-TOSU was added. What's more, tan δ is the ratio of the viscous to the elastic response to an applied force, which argues that resins may become more elastic with the continued addition of DB-TOSU [49]. This result has coincided with the increase in impact strength discussed above.

3.5. LCD 3D printed product and its microstructure analysis

From the above discussion, sample DB-TOSU-30 was selected for the 3D printing application. An LCD 3D printer equipped with an LED light source was used to print complex 3D objects such as a hollow structure, engineering screws, and a biological model without a supporting structure. After 3D printing, the objects were transferred to a UV lightbox for post-curing. The photographs of printed products, engineering screw, and lion model are shown in Figures 9a and 9b, respectively.

All these products are transparent. The hollow structure was printed to observe the printing accuracy, compared with the sample DB-TOSU-0 without the expanding monomer. As shown in Figures 10c and 10e, the hollow structure is printed well by 3D printing resin without or with DB-TOSU. This indicates that the expanding monomer DB-TOSU does not affect

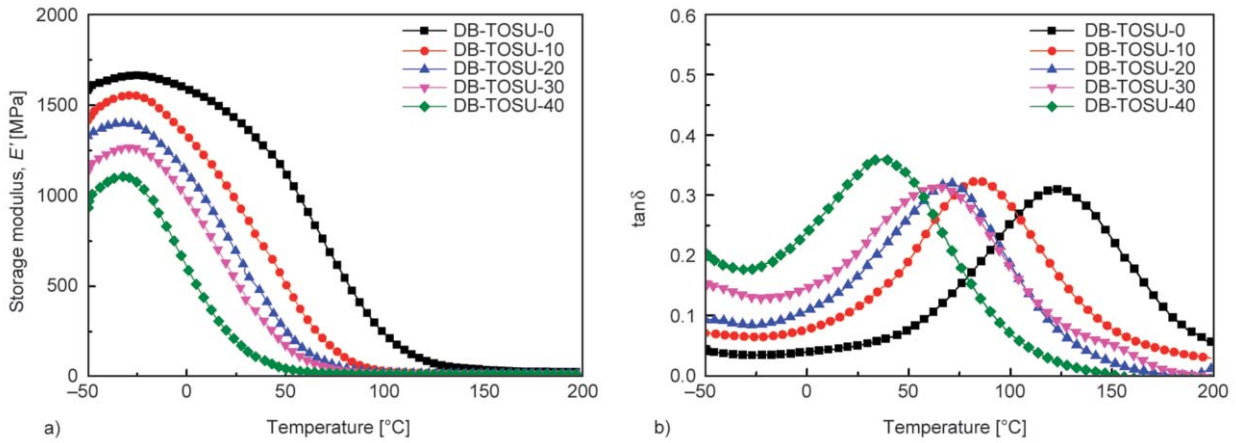

Figure 8. (a) Curves of storage modulus as a function of temperature; (b) curves of loss factor tan δ as a function of temperature.

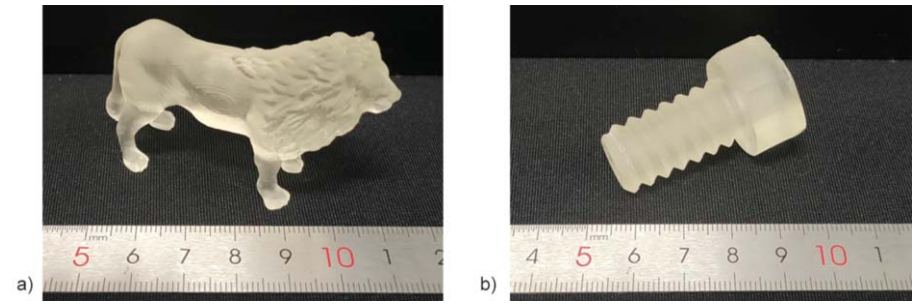

Figure 9. 3D printing of DB-TOSU-30. (a) Lion and (b) engineering screw.

the printing performance of the resin. For the same part of the model, the bar width is 626 μm in SEM micrograph of DB-TOSU-30 in Figure 10d, and it has a deviation of 2.19% compared with 3D model in Figure 10a and Figure 10b. Interestingly, SEM micrograph of DB-TOSU-0 shows a bar width of

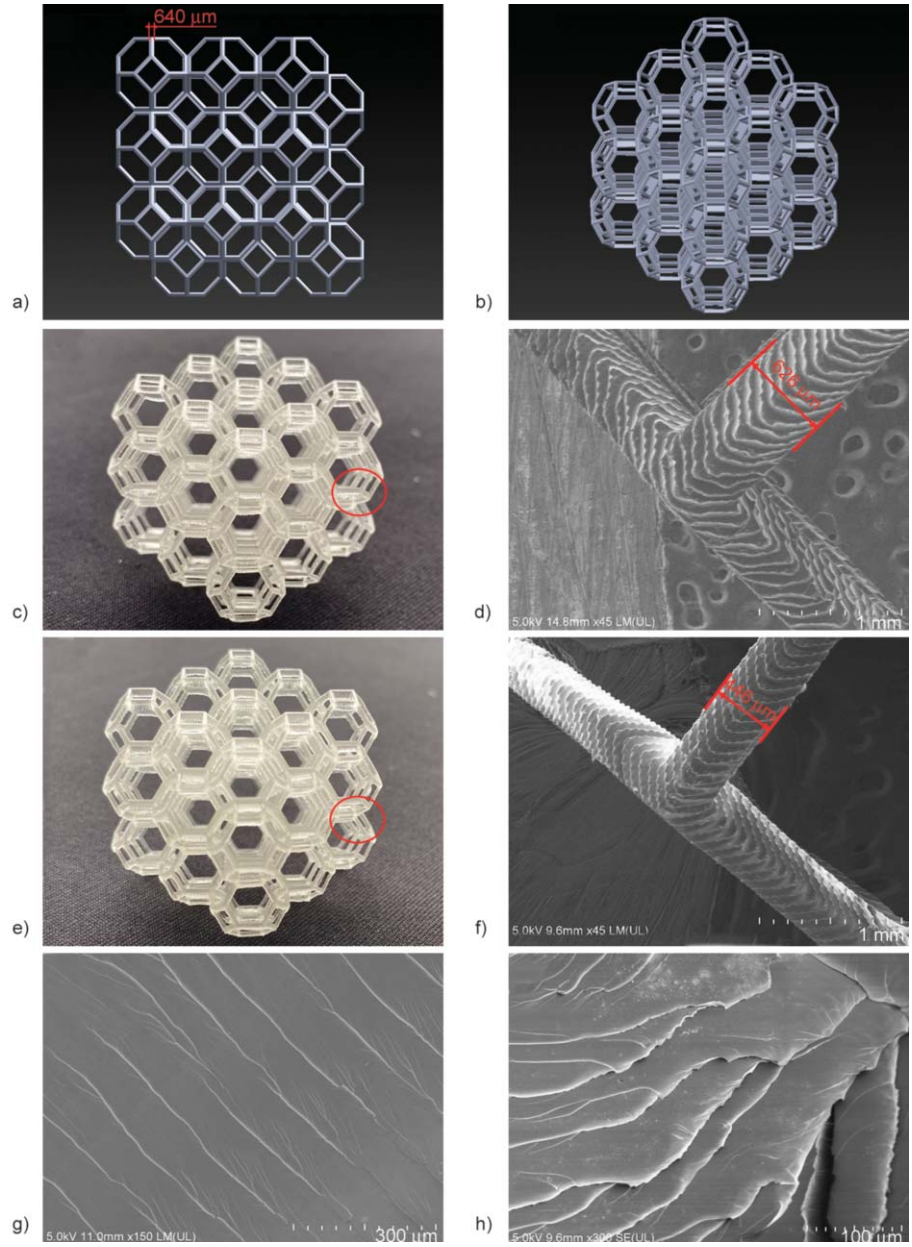

Figure 10. Microstructure of 3D printing products of DB-TOSU-30 and DB-TOSU-0. (a, b) 3D model design by CAD; (c) Hollow structure printed using DB-TOSU-30; (d) SEM micrograph of the hollow structure printed using DB-TOSU-30; (e) hollow structure printed using DB-TOSU-0; (f) SEM micrograph of the hollow structure printed using DB-TOSU-0; (g, h) SEM micrograph of product section printed using DB-TOSU-30.

446 μm in Figure 10f and a deviation of 30.3% compared with 3D model. This distinction comes from the volume shrinkage of pure 3D printing resin during the curing process. Obviously, it illustrates that DB-TOSU can be used as a modifier to effectively reduce the volume shrinkage of 3D printing resin during LCD 3D printing and improve the printing accuracy. On the other hand, DB-TOSU has good compatibility with the printing resin because no phase separation occurs from the SEM micrograph of the product section printed using DB-TOSU-30 in Figures 10g and Figure 10h. Thus, DB-TOSU has a good application prospect in 3D printing owing to its good compatibility with the printing resin and printing accuracy after volume expansion.

4. Conclusions

In this study, SOCs as an additive dealing with volume shrinkage for LCD 3D printing were presented. By RT-FTIR under 405 nm LED light, expanding monomer DB-TOSU was used to study the kinetics of ring-opening photopolymerization. With 5 wt% IRGACURE 204s sensitized by ITX, the ring-opening photopolymerization of spiro group was trigger instantly, and the conversion is up to 84%. As a volume-control agent for LCD 3D printing, volume shrinkage reduction is 71.2% when adding DB-TOSU into 3D printing resin based on SOCs chemistry. The volume shrinkage of the resin with 30 wt% DB-TOSU (DB-TOSU-30) is 0.93%. The toughness of DB-TOSU-30 was enhanced with the maximum impact strength of 2.20 kJ/m^2. Low viscosity characteristics endow DB-TOSU with adaptability and prospect in 3D printing applications. Through a LCD 3D printing application test on DB-TOSU-30, DB-TOSU shows good compatibility with the printing resin from the SEM micrograph. Compared with 3D CAD model, the product printed by DB-TOSU-30 has a bar width deviation of 2.19%, while the product printed by pure resin has a deviation of 30.3%. Thus, based on SOCs chemistry, DB-TOSU as an expanding monomer has a good application prospect in 3D printing.

Acknowledgements

The authors thank the financial support from the Key-Area Research and Development Special Fund Project of Guangdong province (Grants: 2020B090924001 and 2015B010122005) and the National Natural Science Foundation of China (Grants: 51873043).

References

[1] Dall'Argine C., Hochwallner A., Klikovits N., Liska R., Stampf J., Sangermano M.: Hot-lithography SLA-3D printing of epoxy resin. Macromolecular Materials and Engineering, **305**, 2000325/1–2000325/6 (2020). https://doi.org/10.1002/mame.202000325

[2] Shan J., Yang Z., Chen G., Hu Y., Luo Y., Dong X., Zheng W., Zhou W.: Design and synthesis of free-radical/cationic photosensitive resin applied for 3D printer with liquid crystal display (LCD) irradiation. Polymers, **12**, 1346/1–1346/14 (2020). https://doi.org/10.3390/polym12061346

[3] Foli G., Esposti M. D., Morselli D., Fabbri P.: Two-step solvent-free synthesis of poly(hydroxybutyrate)-based photocurable resin with potential application in stereolithography. Macromolecular Rapid Communications, **41**, 1900660/1–1900660/7 (2020). https://doi.org/10.1002/marc.201900660

[4] Jiang Z-H., Li W-D., Yang X., Chen X., Wang C., Chen M-Y., Zhang G-J.: Low dielectric loss and high breakdown strength photosensitive high-k composites containing perfluoroalkylsilane treated $BaTiO_3$ nanoparticles. Composites Part B: Engineering, **192**, 108013/1–108013/9 (2020). https://doi.org/10.1016/j.compositesb.2020.108013

[5] Xiang H., Wang X., Ou Z., Lin G., Yin J., Liu Z., Zhang L., Liu X.: UV-curable, 3D printable and biocompatible silicone elastomers. Progress in Organic Coatings, **137**, 105372/1–105372/11 (2019). https://doi.org/10.1016/j.porgcoat.2019.105372

[6] Li M., Chen Y., Luo W., Cheng X.: Nanoindentation behavior of UV-curable resist and its correlation with patterning defect in nanoimprint lithography. Journal of Micromechanics and Microengineering, **30**, 065010/1–065010/20 (2020). https://doi.org/10.1088/1361-6439/ab87ed

[7] Jian Y., He Y., Jiang T., Li C., Yang W., Nie J.: Volume shrinkage of UV-curable coating formulation investigated by real-time laser reflection method. Journal of Coatings Technology and Research, **10**, 231–237 (2013). https://doi.org/10.1007/s11998-012-9446-2

[8] Yang X., Liu J., Wu Y., Liu J., Cheng F., Jiao X., Lai G.: Fabrication of UV-curable solvent-free epoxy modified silicone resin coating with high transparency and low volume shrinkage. Progress in Organic Coatings, **129**, 96–100 (2019). https://doi.org/10.1016/j.porgcoat.2019.01.005

[9] Cho J-D., Hong J-W.: UV-initiated free radical and cationic photopolymerizations of acrylate/epoxide and acrylate/vinyl ether hybrid systems with and without photosensitizer. Journal of Applied Polymer Science, **93**, 1473–1483 (2004). https://doi.org/10.1002/app.20597

[10] Yang Z., Shan J., Huang Y., Dong X., Zheng W., Jin Y., Zhou W.: Preparation and mechanism of free-radical/cationic hybrid photosensitive resin with high tensile strength for three-dimensional printing applications. Journal of Applied Polymer Science, **138**, 49881/1–49881/11 (2021). https://doi.org/10.1002/app.49881

[11] Tataru G., Coqueret X.: Hybrid free-radical and cationic photo-polymerization of bio-based monomers derived from seed oils – Control of competitive processes by experimental design. Polymer Chemistry, **11**, 5067–5077 (2020). https://doi.org/10.1039/d0py00773k

[12] Exner W., Kühn A., Szewieczek A., Opitz M., Mahrholz T., Sinapius M., Wierach P.: Determination of volumetric shrinkage of thermally cured thermosets using video-imaging. Polymer Testing, **49**, 100–106 (2016). https://doi.org/10.1016/j.polymertesting.2015.11.014

[13] Li Z. Q., Wang C., Qiu W., Liu R.: Antimicrobial thiol–ene–acrylate photosensitive resins for DLP 3D printing. Photochemistry and Photobiology, **95**, 1219–1229 (2019). https://doi.org/10.1111/php.13099

[14] Liu Z., Hong P., Huang Z., Zhang T., Xu R., Chen L., Xiang H., Liu X.: Self-healing, reprocessing and 3D printing of transparent and hydrolysis-resistant silicone elastomers. Chemical Engineering Journal, **387**, 124142/1–124142/13 (2020). https://doi.org/10.1016/j.cej.2020.124142

[15] Bragaglia M., Lamastra F. R., Cherubini V., Nanni F.: 3D printing of polybutadiene rubber cured by photo-induced thiol-ene chemistry: A proof of concept. Express Polymer Letters, **14**, 576–582 (2020). https://doi.org/10.3144/expresspolymlett.2020.47

[16] Song S. Y., Park M. S., Lee D. J., Lee J. W., Yun J. S.: Optimization and characterization of high-viscosity ZrO_2 ceramic nanocomposite resins for supportless stereolithography. Materials and Design, **180**, 107960/1–107960/9 (2019). https://doi.org/10.1016/j.matdes.2019.107960

[17] Zheng T., Ni X.: Improving the stability of UV-cured materials by the radical scavenger loaded into halloysite nanotubes. Journal of Nanoscience and Nanotechnology, **18**, 6815–6822 (2018). https://doi.org/10.1166/jnn.2018.15522

[18] Li N., Liu Y., Fang C., Lu G.: Epoxy acrylate modified by talc in three dimensional printing. Materials Research Express, **5**, 085306/1–085306/9 (2018). https://doi.org/10.1088/2053-1591/aad0df

[19] Contreras P. P., Kuttner C., Fery A., Stahlschmidt U., Jérôme V., Freitag R., Agarwal S.: Renaissance for low shrinking resins: All-in-one solution by bi-functional vinylcyclopropane-amides. Chemical Communications, **51**, 11899–11902 (2015). https://doi.org/10.1039/c5cc03901k

[20] Seidler K., Griesser M., Kury M., Harikrishna R., Dorfinger P., Koch T., Svirkova A., Marchetti-Deschmann M., Stampfl J., Moszner N., Gorsche C., Liska R.: Vinyl sulfonate esters: Efficient chain transfer agents for the 3D printing of tough photopolymers without retardation. Angewandte Chemie International Edition, **57**, 9165–9169 (2018). https://doi.org/10.1002/anie.201803747

[21] Ortiz R. A., Gomez A. G. S., Valdez A. E. G., Flores R. A., Sangermano M.: Development of low-shrinkage polymers by using expanding monomers. Macromolecular Symposia, **374**, 1600092/1–1600092/6 (2017). https://doi.org/10.1002/masy.201600092

[22] Nemoto N., Sanda F., Endo T.: Cationic ring-opening polymerization of six-membered cyclic carbonates with ester groups. Journal of Polymer Science Part A: Polymer Chemistry, **39**, 1305–1317 (2001). https://doi.org/10.1002/pola.1108

[23] Sangermano M., Ortiz R. A., Urbina B. A. P., Duarte L. B., Valdez A. E. G., Santos R. G.: Synthesis of an epoxy functionalized spiroorthocarbonate used as low shrinkage additive in cationic UV curing of an epoxy resin. European Polymer Journal, **44**, 1046–1052 (2008). https://doi.org/10.1016/j.eurpolymj.2008.01.039

[24] Ortiz R. A., Duarte M. L. B., Gómez A. G. S., Sangermano M., Valdez A. E. G.: Novel diol spiro orthocarbonates derived from glycerol as anti-shrinkage additives for the cationic photopolymerization of epoxy monomers. Polymer International, **59**, 680–685 (2010). https://doi.org/10.1002/pi.2755

[25] Ortiz R. A., Medina L. A. R., Duarte M. L. B., Samaniego L. I., Valdez A. E. G., Mendez Z. L. G., Gonzalez L. M.: Synthesis of glycerol-derived diallyl spiroorthocarbonates and the study of their antishrinking properties in acrylic dental resins. Journal of Materials Science: Materials in Medicine, **24**, 2077–2084 (2013). https://doi.org/10.1007/s10856-013-4959-5

[26] Min H., Zheng N., Fan Z., Jiang Y., Cheng X.: UV-curable nanoimprint resist with liquid volume-expanding monomers. Microelectronic Engineering, **205**, 32–36 (2019). https://doi.org/10.1016/j.mee.2018.10.011

[27] Marx P., Romano A., Roppolo I., Chemelli A., Mühlbacher I., Kern W., Chaudhary S., Andritsch T., Sangermano M., Wiesbrock F.: 3D-printing of high-κ thiol-ene resins with spiro-orthoesters as anti-shrinkage additive. Macromolecular Materials and Engineering, **304**, 1900515/1–1900515/10 (2019). https://doi.org/10.1002/mame.201900515

[28] Xiang H., Wang X., Lin G., Xi L., Yang Y., Lei D., Dong H., Su J., Cui Y., Liu X.: Preparation, characterization and application of UV-curable flexible hyperbranched polyurethane acrylate. Polymers, **9**, 552/1–552/12 (2017). https://doi.org/10.3390/polym9110552

[29] Nguyen T. V., Nguyen-Tri P., Azizi S., Dang T. C., Hoang D. M., Hoang T. H., Nguyen T. L., Bui T. T. L., Dang V. H., Nguyen N. L., Le T. T., Nguyen T. N. L., Vu Q. T., Tran D. L., Dang T. M. L., Lu L. T.: The role of organic and inorganic UV-absorbents on photopolymerization and mechanical properties of acrylate-urethane coating. Materials Today Communications, **22**, 100780/1–100780/8 (2020). https://doi.org/10.1016/j.mtcomm.2019.100780

[30] Yoo S. H., Park K., Kim J., Kim C. K.: Characteristics of dental restorative composites fabricated from bis-GMA alternatives and spiro orthocarbonates. Macromolecular Research, **19**, 27–32 (2011). https://doi.org/10.1007/s13233-011-0115-6

[31] Takata T., Ariga T., Endo T.: Cationic ring-opening polymerization of five-membered spiro orthocarbonates: Unsubstituted and 2,8-diaryl-1,4,6,9-tetraoxaspiro[4.4]nonanes. Macromolecules, **25**, 3829–3833 (1992). https://doi.org/10.1021/ma00041a001

[32] Wang T., Ma L. J., Wan P. Y., Liu J. P., Wang F.: A study of the photoactivities and thermomechanical properties of epoxy resins using novel [cyclopentadien-Fe-arene]$^{+}$ PF_6^{-} photoinitiators. Journal of Photochemistry and Photobiology A: Chemistry, **163**, 77–86 (2004). https://doi.org/10.1016/s1010-6030(03)00432-5

[33] Nesmeyanov A. N., Vol'kenau N. A., Boleaova I. N.: The interaction of ferrocene and its derivatives with aromatic compounds. Tetrahedron Letters, **4**, 1725–1729 (1963). https://doi.org/10.1016/s0040-4039(01)90903-7

[34] Wang T., Li B. S., Zhang L. X.: Carbazole-bound ferrocenium salt as an efficient cationic photoinitiator for epoxy polymerization. Polymer International, **54**, 1251–1255 (2005). https://doi.org/10.1002/pi.1837

[35] Esen H., Barghorn C. C., Allonas X.: Light induced gradient refractive index materials. Polymers for Advanced Technologies, **27**, 66–72 (2016). https://doi.org/10.1002/pat.3598

[36] Lin Y., Stansbury W. J.: Kinetics studies of hybrid structure formation by controlled photopolymerization. Polymer, **44**, 4781–4789 (2003). https://doi.org/10.1016/S0032-3861(03)00469-5

[37] Crivello J. V., Kong S.: Synthesis and characterization of second-generation dialkylphenacylsulfonium salt photoinitiators. Macromolecules, **33**, 825–832 (2000). https://doi.org/10.1021/ma991661n

[38] Khudyakov I. V.: Fast photopolymerization of acrylate coatings: Achievements and problems. Progress in Organic Coatings, **121**, 151–159 (2018). https://doi.org/10.1016/j.porgcoat.2018.04.030

[39] Dektar J. L., Hacker N. P.: Photochemistry of diaryliodonium salts. The Journal of Organic Chemistry, **55**, 639–647 (1990). https://doi.org/10.1021/jo00289a045

[40] Chen Z., Webster D. C.: Study of cationic UV curing and UV laser ablation behavior of coatings sensitized by novel sensitizers. Polymer, **47**, 3715–3726 (2006). https://doi.org/10.1016/j.polymer.2006.03.091

[41] Jahn R., Jung T.: Relationship between pigment properties and UV-curing efficiency. Progress in Organic Coatings, **43**, 50–55 (2001). https://doi.org/10.1016/s0300-9440(01)00221-1

[42] Li Z., Chen H., Wang C., Chen L., Liu J., Liu R.: Efficient photopolymerization of thick pigmented systems using upconversion nanoparticles-assisted photochemistry. Journal of Polymer Science Part A: Polymer Chemistry, **56**, 994–1002 (2018). https://doi.org/10.1002/pola.28969

[43] Höfer M., Liska R.: Photochemistry and initiation behavior of phenylethynyl onium salts as cationic photoinitiators. Journal of Polymer Science Part A: Polymer Chemistry, **47**, 3419–3430 (2009). https://doi.org/10.1002/pola.23423

[44] Han J., Jiang S., Gao Y., Sun F.: Intramolecular-initiating photopolymerization behavior of nanogels with the capability of reducing shrinkage. Journal of Materials Chemistry C, **4**, 10675–10683 (2016). https://doi.org/10.1039/c6tc03839e

[45] Kostoryz E. L., Tong P. Y., Chappelow C. C., Glaros A. G., Eick J. D., Yourtee D. M.: In vitro toxicity of spiro-orthocarbonate monomers designed for non-shrinking dental restoratives. Journal of Biomaterials Science Polymer Edition, **11**, 187–196 (2000). https://doi.org/10.1163/156856200743643

[46] Li S., Sun D., Li A., Cui Y.: Study on curing shrinkage and mechanism of DHOM-modified epoxy-acrylate-based UV-curing 3D printing materials. Journal of Applied Polymer Science, **138**, 49859/1–49859/9 (2021). https://doi.org/10.1002/app.49859

[47] Zhou S-Y., Zhu L-R., Wang M-D.: Research on probability of seismic critical instability on basis of 'fracture collusion' model. Acta Seismologica Sinica, **11**, 473–478 (1998). https://doi.org/10.1007/s11589-998-0093-8

[48] Horigome K., Ebe K., Kuroda S-I.: UV curable pressure-sensitive adhesives for fabricating semiconductors. II. The effect of functionality of acrylate monomers on the adhesive properties. Journal of Applied Polymer Science, **93**, 2889–2895 (2004). https://doi.org/10.1002/app.20884

[49] Marx P., Romano A., Fischer R., Roppolo I., Sangermano M., Wiesbrock F.: Dual-cure coatings: Spiroorthoesters as volume-controlling additives in thiol–ene reactions. Macromolecular Materials and Engineering, **304**, 1800627/1–1800627/5 (2019). https://doi.org/10.1002/mame.201800627

[50] Chiappone A., Jeremias S., Bongiovanni R., Schönhoff M.: NMR study of photo-crosslinked solid polymer electrolytes: The influence of monofunctional oligoethers. Journal of Polymer Science Part B: Polymer Physics, **51**, 1571–1580 (2013). https://doi.org/10.1002/polb.23371

[51] Suliga A., Jakubczyk E. M., Hamerton I., Viquerat A.: Analysis of atomic oxygen and ultraviolet exposure effects on cycloaliphatic epoxy resins reinforced with octa-functional POSS. Acta Astronautica, **142**, 103–111 (2018). https://doi.org/10.1016/j.actaastro.2017.10.018